JOURNAL OF MOLECULAR SPECTROSCOPY 139, 126–146 (1990)

Critical Phenomena and Diabolic Points in Rovibrational Energy Spectra of Spherical Top Molecules

V. M. KRIVTSUN AND D. A. SADOVSKII

Institute of Spectroscopy, USSR Academy of Sciences, Troitzk, Moscow Region 142092, USSR

AND

B. I. ZHILINSKII

Chemistry Department, Moscow State University, Moscow 119899, USSR

The qualitative modifications of the rovibrational energy-level structure under rotational excitation are studied for spherical top molecules. The ν_2, ν_4 bands of $^{12}CD_4$ and $^{120}SnH_4$ and the ν_1, ν_3 bands of $^{120}SnH_4$ are treated as examples. Two types of qualitative changes are shown to exist: the critical phenomena corresponding to the modification of the cluster structure and the so-called diabolic points associated with the redistribution of energy levels between different branches as the rotational quantum number increases. A simple model interpretation of energy-level redistribution is given to show that such a phenomenon is typical for tetrahedral molecules. Manifestation of critical phenomena and diabolic point formation in high-resolution infrared spectra are discussed.

1. INTRODUCTION

The qualitative description of high-resolution experimental data on rovibrational molecular spectra is based nowadays on the utilization of complicated effective Hamiltonians with large numbers of phenomenological parameters, i.e., spectroscopic constants. Such an approach encounters obvious technical obstacles for excited vibrational states due to a sharp increase of the number of resonant vibrational states and the number of effective parameters as well. The simplification of this problem can be achieved if regular sequences of states are indicated within the rotational multiplet of the vibrational polyad considered. From this point of view, the classical analysis of rotational motion proves very useful. It enables one to find in the rotational level system the localized states corresponding in the classical limit to the small precession of the angular momentum around some stable rotation axes (*1–9*). Such quantum states form the regular sequences of the quasidegenerate levels (the so-called clusters). Besides clusters, the quantum energy spectrum shows the existence of states with essentially delocalized wavefunctions. These quantum states correspond to an unstable classical rotation and are situated in the energy region between clusters of different types. Such a simple classical analysis which clearly explains the rotational cluster structure has been widely discussed in the literature, especially for spherical top molecules (*1–6*).

0022-2852/90 $3.00

The cluster structure reflects the rotational dynamics of the molecules. The rotational excitation may result in modifications of the dynamical behavior and the corresponding cluster structure. As shown in Refs. (*8, 9*), modifications of the cluster structure can be interpreted as critical phenomena associated in the classical limit with the formation or disappearance of new stable rotation axes. The phenomenological (Landau type) theory of the classical phenomena in the rotational spectra of finite particle systems was presented recently (*8, 9*), but the demonstration of such phenomena by analysis of the experimental data is not yet given.

Spherical top molecules are extremely suitable for the study of qualitative features of rotational energy levels due to rich information on the rovibrational energy levels of these molecules and to the high density of rotational and vibrational states which results in a rather complicated energy-level system. Degenerate and quasidegenerate vibrational states are typical for spherical tops. Thus, along with critical phenomena, another type of qualitative effect is appropriate for the same molecules: the redistribution of rotational energy levels between different branches in the energy spectra. This phenomenon was shown to be related in the classical limit to the formation of the conical intersection points (or diabolic points) of different rotational energy surfaces (*12, 16*). Such a situation is typical for quantum problems with intersecting rotational multiplets. It should be noted that the qualitative phenomena associated with the formation of diabolic points either in the space of parameters or in the space of dynamic variables are appropriate for very different physical problems (*10–12*).

This article is devoted to the study of both types of qualitative effects for energy-level systems of real spherical top molecules. Section 2 gives a brief outline of the general semiclassical analysis appropriate for the study of qualitative effects. The study of diabolic points for the ν_2, ν_4 bands of tetrahedral molecules is taken up in Section 3. The critical phenomena in the ν_2 band are studied in detail in Section 4 through an analysis of experimental data on $^{120}SnH_4$ (*13*). Section 5 deals with the qualitative analysis of new experimental data on the ν_1, ν_3 bands of $^{120}SnH_4$ (*14*). The existence of the diabolic point connected with the intersection of the ν_1 and ν_3 bands and the existence of the critical phenomenon in the F^0-branch of the ν_3 band, which is analogous to that found in the ν_2, ν_4 dyad, are shown. This special interest in the ν_1, ν_3 bands of $^{120}SnH_4$ is due to the fact that particular attention was paid during the experimental investigation to the part of the energy spectrum exhibiting the critical behavior. Thus, the manifestation of the critical phenomenon in the experimental spectra is specially discussed.

2. ENERGY SPECTRUM OF THE EFFECTIVE OPERATOR IN THE CLASSICAL LIMIT

Transformation of the effective quantum operator into its classical analog enables one to easily realize the qualitative analysis of the problem considered and, in particular, the qualitative changes associated with the variation of such an important physical parameter as the total angular momentum $|J| = (J(J+1))^{1/2}$. Transformation to the classical limit may be made using the well-known simple formulae

$$J_z = |J|\cos(\theta), \qquad J_x = |J|\cos(\phi)\sin(\theta), \qquad J_y = |J|\sin(\phi)\sin(\theta). \quad (1)$$

In this case the effective rotational Hamiltonian of a general type,

$$H_{\text{rot}} = \sum_{a,b,c} C_{abc}(J_x^a J_y^b J_z^c + \text{c.c.}) = H(J_x, J_y, J_z), \tag{2}$$

has as its classical analog the scalar function $E^J(\theta, \phi)$ depending on two dynamic variables, θ, ϕ and the phenomenological spectroscopic constants C_{abc}. The function $E^J(\theta, \phi)$ is usually called the rotational energy surface (*6*). The angles θ, ϕ specify the direction of the classical rotation axis and play the role of classical phase variables. The qualitative analysis of the rotational energy surface $E^J(\theta, \phi)$ includes first the location of the stationary points and the study of their stability. The maxima and minima of the energy surface $E^J(\theta, \phi)$ correspond to the stable rotation axes in the classical problem and to a sequence of localized states in the associated quantum problem. The stability of the rotation around any given axis can be estimated qualitatively using the Hessian value

$$\left(\frac{\partial^2 E^J}{\partial \phi^2} + \frac{\partial^2 E^J}{\partial \theta^2} - \frac{\partial^2 E^J}{\partial \phi \partial \theta}\right) \Big/ \sin^2 \theta. \tag{3}$$

Localized quantum states with a high value of the projection of the angular momentum on a given axis are only formed if the Hessian is positive and sufficiently large. For high Hessian values the regular sequence of the quantum states can exist. It is well characterized by the good quantum number $M = J, J-1, \ldots$, the projection of the angular momentum on the stable rotation axis. Symmetry requirements result in the fact that a system of equivalent stationary points generally exists for the energy surface $E^J(\theta, \phi)$ of spherical top molecules. For example, in the case of a cubic rotational symmetry group there are 6, 8, and 12 equivalent stationary points corresponding, respectively, to the C_4, C_3, and C_2 rotation axes. In this case, the localized quantum states form quasidegenerate groups, the so-called clusters, which are widely discussed in the literature (*1–6*). The rotational multiplets of spherical top molecules, in particular the rotational structure of the ground vibrational state, are generally characterized by regular sequences of 6-fold and 8-fold clusters. Intracluster splitting usually decreases exponentially as the cluster energy approaches the limiting classical value. The splitting becomes smaller for higher Hessian values as well. The symmetry types of the levels forming each cluster can easily be found from induced representation theory taking into account the local symmetry group **g** for the stationary rotation axes (*2, 15*).

Let us consider now the quantum number J of the angular momentum as a parameter. In this case a natural question arises: what are the generic qualitative changes of the rotational energy surface under J variation, i.e., under rotational excitation? The clearest visualization of the qualitative changes can be achieved by plotting the energies at the stationary points of the energy surface in (E, J) variables (*8, 9*). This energy (or bifurcation) diagram shows the formation (or disappearance) of stationary points and, consequently, indicates modifications in the cluster structure of the rotational multiplet. To complete the energy diagram it is useful to indicate the Hessian values for all stationary points. The sign of the Hessian shows the stability of the stationary point and the possibility of the formation (in principle) of the sequence of localized states (the clusters) of a given type. A negative Hessian value corresponds

to an unstable rotation. A zero value of the Hessian for some critical value J_c of the angular momentum indicates bifurcation in the limiting classical problem. The bifurcation is associated with qualitative modification of a system of stationary points of the energy surface and with variation of the topological structure of the set of classical phase trajectories. The corresponding phenomena taking place for the parent quantum problem at $J \sim J_c$ were called in Ref. (*8*) the critical ones. In Ref. (*8*) the general classification of the critical phenomena in an isolated rotational multiplet was given. It is based on the notion of the local symmetry group **g**. Five different types of critical phenomena are possible for a pure rotational problem in the case of finite symmetry groups (*8*): nonlocal critical phenomenon with the C_1 local symmetry group, local and nonlocal critical phenomena with the C_2 local symmetry group, nonlocal critical phenomena appropriate for the C_3 and C_4 local symmetry groups, and local critical phenomena appropriate for C_n ($n > 3$) local symmetry groups. The manifestation of the critical phenomena in the energy-level system of the quantum problem is the modification of the cluster structure. For example, the nonlocal C_2 critical phenomenon in the case of spherical top molecules corresponds to the formation or disappearance of 12-fold clusters in the energy spectra due to the transformation of an unstable stationary C_2 axis into a stable one or vice versa during the corresponding classical bifurcation.

The model of an isolated nondegenerated vibrational state is acceptable for polyatomic molecules in a very limited number of cases. The existence of degenerate vibrations and polyads of resonant vibrational states requires the explicit introduction of rovibrational interactions. The natural generalization of the effective rotational Hamiltonian in this case is the effective rotation–vibration Hamiltonian which may be written in a matrix form as

$$H_{\text{vib-rot}} = \begin{pmatrix} H_{11}(J_x, J_y, J_z) & \cdots & H_{1N}(J_x, J_y, J_z) \\ \cdots & \cdots & \cdots \\ H_{N1}(J_x, J_y, J_z) & \cdots & H_{NN}(J_x, J_y, J_z) \end{pmatrix}, \tag{4}$$

where N is the number of resonance vibrational states forming the polyad and the matrix elements $H_{ij}(J_x, J_y, J_z)$ can be expanded, similarly to (2), in proper series taking into account the symmetry requirements and hermiticity. Similarly to the Hamiltonian (2) the quantum number J for the operator (4) is an integral of motion and the phase space for the limiting classical problem is two-dimensional sphere. At the same time the classical symbol for the Hamiltonian (4) is now the Hermitian matrix

$$H^J_{\text{vib-rot}} = \begin{pmatrix} H^J_{11}(\theta, \phi) & \cdots & H^J_{1N}(\theta, \phi) \\ \cdots & \cdots & \cdots \\ H^J_{N1}(\theta, \phi) & \cdots & H^J_{NN}(\theta, \phi) \end{pmatrix}, \tag{5}$$

which can easily be obtained from (4) using the expressions (1). This approach was called semiclassical in Ref. (*3, 16*) due to simultaneous use of the classical description

for the rotational degrees of freedom and the quantum description for the vibrational motion.

The eigenvalues of the matrix (5) are to be interpreted as rotational energy surfaces $E_k^J(\theta, \phi)$ for each vibrational state of a polyad ($k = 1, \ldots, N$). These energy surfaces may be interpreted as N deformed spheres put one into another. The qualitative study of the rotational structure of the polyad reduces in the classical limit to the bifurcation analysis of each energy surface $E_k^J(\theta, \phi)$. At the same time, an additional possibility of the appearance of a new qualitative phenomenon exists for a system of energy surfaces. Two rotational energy surfaces can form a conical intersection point (the so-called diabolic point). This means that for an isolated value $J = J_c$ two surfaces form one two-sheet surface. Such a situation, for example, naturally arises in the case of the quantum problem with intersecting rotational multiplets of different vibrational states. One can note that the behavior of the Hessian value at $J \to J_c$ depends obviously on the local symmetry group **g** of the corresponding diabolic point. If this symmetry group is C_n, $n = 3, 4, \ldots$, stable stationary points exist at $J \neq J_c$ on both energy surfaces and in consequence the Hessian value is positive.

It was shown in Ref. (*12*) that the formation of a diabolic point for a classical symbol reflects such qualitative phenomena in the energy spectrum of the quantum problem as the redistribution of the energy levels between different branches. This phenomenon is a purely quantum one because a simple semiclassical quantization procedure for separated isolated energy surfaces cannot yield a state with the energy close to the diabolic point. Such a highly localized state may exist only due to quantum tunneling between different energy surfaces and it is just this state that goes from one branch to another passing through the diabolic point with J variation.

It should be noted that for spherical top molecules the formation of a system of diabolic points takes place simultaneously at a number of symmetry equivalent points (6, 8, 12, $\cdots$) depending on their local symmetry group. Accordingly, the redistribution of the 6, 8, 12, $\cdots$-fold clusters between different branches takes place with an increasing J. The relation between diabolic point formation for the rovibrational problem and some other problems in very different fields of physics (particle and nuclear physics, superconductivity, light propagation, etc.) was briefly discussed in Ref. (*12*), where the interpretation of the redistribution phenomena in terms of Berry's geometrical phase (*10, 11*) was given. The mathematical reason is the topological origin of the diabolic point. It shows, consequently, the independence of this phenomenon of the concrete form of the Hamiltonian.

3. DIABOLIC POINTS IN THE ROTATIONAL STRUCTURE OF THE ν_2, ν_4 DYAD OF TETRAHEDRAL MOLECULES

The ν_2, ν_4 dyad of bending modes in tetrahedral molecules is an example of the most widely studied vibrational polyads. The separation between the ν_2 and ν_4 bands of CH_4, CD_4, SiH_4, and GeH_4 is about 100–200 cm^{-1}. Thus, the description of the rotational structure in terms of isolated vibrational bands is possible for $J < 10$ only. For higher J values explicit introduction of the resonance interaction terms is necessary. The most important nondiagonal Coriolis interaction term, $\mathbf{U}_{2,4}^{1(1,F_1)}$, was first introduced in Ref. (*17*). Much more elaborate resonance models are successfully used now

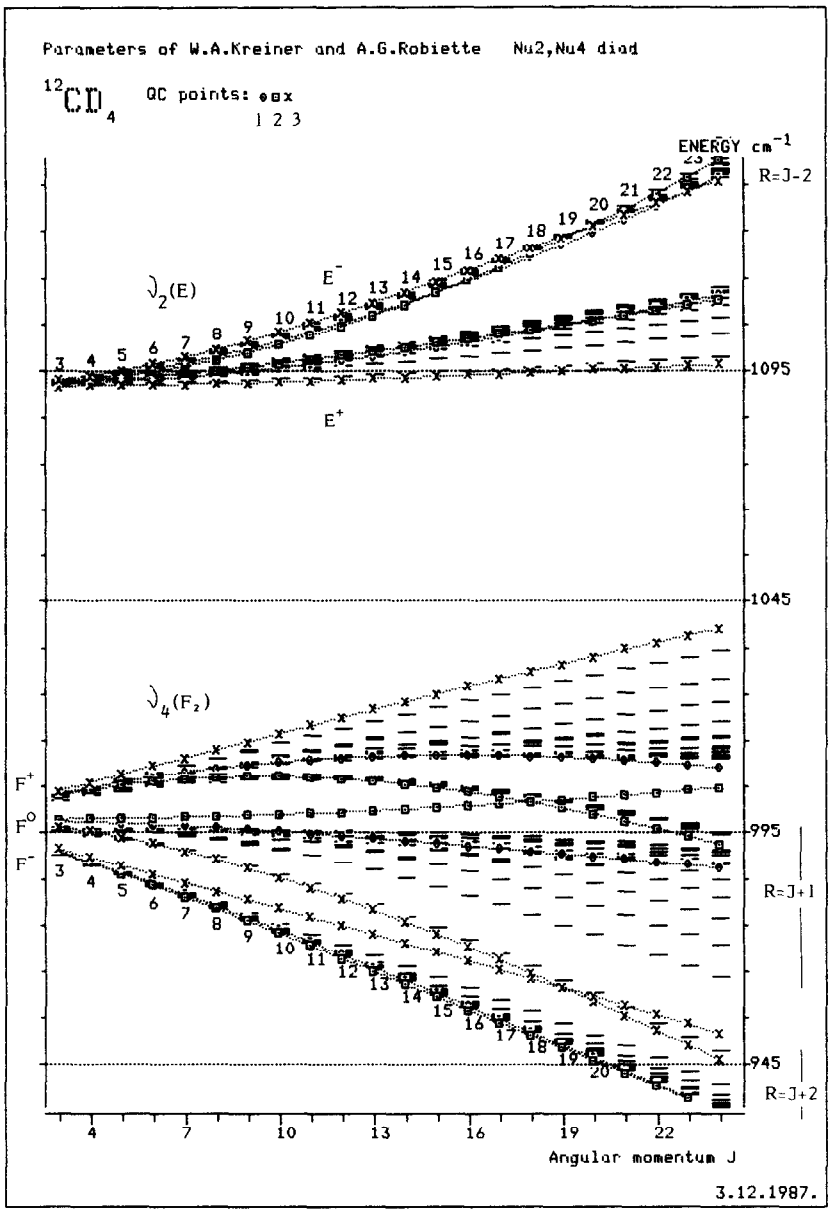

FIG. 1. The rotational structure of the ν_2, ν_4 dyad of $^{12}CD_4$ calculated according to the parameters of Ref. (*19*). The dashed line indicates the classical rotation energy around stationary axes: (1) C_2 (rhomb); (2) C_3 (square); (3) C_4 (cross). *Note*: The energy of the rotational states is given after the scalar part of the ground state energy is subtracted: $E - (B_0J(J+1) - D_0J^2(J+1)^2 + \cdots)$.

for the analysis of the ν_2, ν_4 bands of many tetrahydrides (*18*). Figure 1 shows the rotational structure of the ν_2, ν_4 dyad of $^{12}CD_4$ calculated from the data of Ref. (*19*). The rotational multiplet includes five well-separated branches corresponding to five

vibrational levels of the dyad ($\nu_2(E)$ is doubly degenerate and $\nu_4(F_2)$ is triply degenerate). This structure is typical for almost all tetrahedral molecules and is mainly due to the frequency difference $\Delta = \nu_2 - \nu_4$ and the Coriolis interaction given up to the first order by two independent parameters $u_{4,4}^{1(1,F_1)}$ and $u_{2,4}^{1(1,F_1)}$. For low J values ν_4 shows a well-known three-branch structure: F^+, F^0, F^- (*20*), caused by diagonal Coriolis interaction $\mathbf{U}_{4,4}^{1(1,F_1)}$. The ν_2 band includes two branches which are formed due to resonance Coriolis interaction with the ν_4 band and diagonal interactions of higher orders, $\mathbf{U}_{2,2}^{2(2,E)}$, etc. For higher J values the $\Delta\nu$ value is of the same order as the Coriolis interaction. This results in the redistribution of the energy levels between different branches of the rotational multiplet. Figure 1 clearly shows the transition of an 8-fold cluster from the upper F^+ branch of the ν_4 band to the F^0 band and the transition of a 6-fold cluster from F^0 to F^- with an increase of J. In addition to quantum energy levels, Fig. 1 shows the results of classical analysis of the ν_2, ν_4 dyad. Classical energies for stationary points with the C_2, C_3, and C_4 local symmetry are only shown for the sake of simplicity. It is clear from the diagram that the conical intersection of the rotational energy surfaces for the F^+ and F^0 branches takes place at $J \sim 18$ in the direction of the C_3 axis. Indeed, due to symmetry there are eight equivalent diabolic points which cause the redistribution of the 8-fold cluster between these two branches. Another diabolic point occurs at $J \sim 19$ between the F^0 and F^- branches in the direction of the C_4 axis. It results in regrouping of the 6-fold cluster.

The redistribution of the energy levels is so obvious that for $J > 20$ it seems to be natural to introduce a new pseudorotational quantum number R which takes values $R = J + 2$ and $R = J + 1$ for the lowest and central branches of the ν_4 band and describes the numbers of the energy levels in these branches as equal to $2R + 1$. The appearance of new well-separated branches evidences the modification of the dynamical symmetry of the problem considered, which can be interpreted as the recoupling of the vibrational and rotational angular momenta.

Let us now give a qualitative explanation of this phenomenon. First of all, we neglect the tetrahedral splitting and suppose that the dynamical symmetry for the quickly rotating molecule is close to spherical. To realize such a supposition we use the Hamiltonian, which is invariant with respect to the $SO(3)$ group. The relevant details are given in the Appendix. We note only that five vibrational operators,

$$(\mathbf{a}_2)_1^E, (\mathbf{a}_2)_2^E, (\mathbf{a}_4)_x^{F_2}, (\mathbf{a}_4)_y^{F_2}, (\mathbf{a}_4)_z^{F_2},$$

must be considered as components of the spherical tensor of rank two. For the spherically invariant Hamiltonian, only one term linear in angular momentum operators is admissible: the operator $\mathbf{H}_1$ in the expression (A-5).

$$\mathbf{H}_1^{(SO(3))} = (\mathbf{U}_{4,4}^{1(1,F_1)} - 2^{1/2}\mathbf{U}_{2,4}^{1(1,F_1)})/5^{1/2}.$$

As soon as the first-order Coriolis interaction is responsible for the branch structure of the rotational multiplet, the $SO(3)$ invariant tensor operator $\mathbf{H}_1$ is the most important one for the qualitative interpretation of the branch structure. Its spectrum includes five branches characterized by the pseudorotational quantum number R: $R = J + 2, J + 1, \ldots, J - 2$. Each branch includes $(2R + 1)$ degenerate levels (we neglect the $(2J + 1)$-fold degeneracy with respect to the projection of the total angular momentum on the laboratory fixed frame (*21, 22*)). It can easily be verified that the

branches in the spectrum of the operator $\mathbf{H}_1$ are similar to those appropriate for the ν_2, ν_4 dyad at high J values. To describe properly the main effect appropriate to the $SO(3)$ symmetry violation, we consider the model problem with the Hamiltonian

$$\mathbf{H} = (\Delta/2)\mathbf{H}_0^{(T_d)} + t\mathbf{H}_1^{(SO(3))},$$

$$\mathbf{H}_0^{(T_d)} = 2^{1/2}\mathbf{U}_{2,2}^{0(0,A_1)} - 3^{1/2}\mathbf{U}_{4,4}^{0(0,A_1)} = \sum_{s=1,2} (\mathbf{a}_2^+)_s^E(\mathbf{a}_2)_s^E - \sum_{s=1,3} (\mathbf{a}_4^+)_s^{F_2}(\mathbf{a}_4)_s^{F_2}. \quad (6)$$

The term $\mathbf{H}_1^{(SO(3))}$ in Eq. (6) possesses spherical symmetry and describes the Coriolis interactions. The $\mathbf{H}_0$ term describes the resonance detuning between the ν_2 and ν_4 states which results in broken spherical symmetry for $\Delta \neq 0$. The energy level system for the Hamiltonian (6) is shown in Fig. 2 together with the result of the semiclassical analysis. It is clearly seen from Fig. 2 that the Hamiltonian (6) adequately reproduces the redistribution of the energy levels between the branches of the ν_2, ν_4 dyad under rotational excitation. The transition to the new scheme of the coupling of the rotational and vibrational angular momenta in the case of operator (6) is completed by passing the 6-fold cluster from the lower ν_2 branch to the ν_4 state. In the CD_4 molecule this transition probably takes place for rather high J-values due to a large value of $\Delta\nu$. The example of the ν_2, ν_4 dyad of $^{28}SiH_4$ shows such a transition much more clearly. The phenomenon of energy-level redistribution between different branches of the ν_2, ν_4 bands is also appropriate for some other tetrahedral molecules. This supposition follows from the analysis of the parameters of the first-order Coriolis interaction, $u_{2,4}^{1(1,F_1)}$ and $u_{4,4}^{1(1,F_1)}$. According to Eq. (A-5), if spherical symmetry is required these parameters must satisfy the relation

$$u_{2,4}^{1(1,F_1)} = -2^{1/2}u_{4,4}^{1(1,F_1)}. \quad (7)$$

Table I shows that Relation (7) is approximately correct for a number of molecules and is most accurate for the CD_4 and SiH_4.

4. THE CRITICAL PHENOMENA IN THE ROTATIONAL STRUCTURE OF TETRAHEDRAL MOLECULES: $\nu_2(E)$ VIBRATIONAL STATE

Let us now study the cluster structure of the rotational levels of the ν_2, ν_4 dyad. To describe properly this complicated rotational structure, a number of rovibrational tensor operators should be introduced into the Hamiltonian. As the degree of the elementary rotational operators J_a ($a = x, y, z$) is different for various terms, the relative contributions of these terms depend strongly on the rotational quantum number. Each tensor operator may be characterized by the system of stationary axes and by its own cluster structure correspondingly. Thus, from the known set of the spectroscopic parameters it is almost impossible to predict (without numerical calculations) the rotational cluster structure even approximately due to the dependence of the high-order contributions on the value of J and the rearrangement of the cluster structure of the rotational multiplet as J increases. Such a rearrangement (or *perestroika*) is associated with the critical phenomena discussed above in Sect. 2. For spherical tops the simplest example of this kind is given by the well-known model Hamiltonian of the ground state,

$$\mathbf{H}_{\text{rot}} = u_0^{4(4,A_1)}\mathbf{R}^{4(4,A_1)} + u_0^{6(6,A_1)}\mathbf{R}^{6(6,A_1)} + \text{scalar terms}. \quad (8)$$

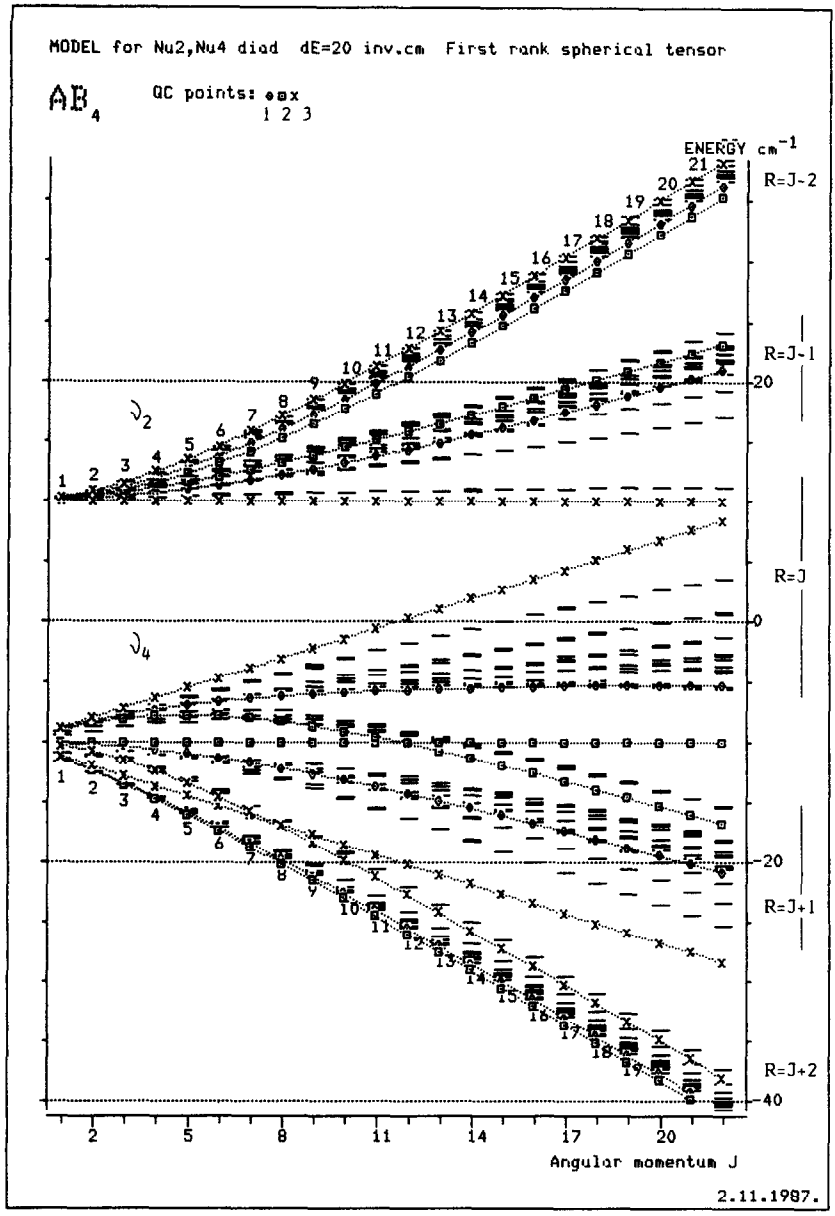

FIG. 2. The rotational structure of the model Hamiltonian including the two most important terms responsible for the rotational structure of the ν_2, ν_4 dyad of tetrahedral molecules. The dashed line indicates the classical rotation energy around stationary axes: (1) C_2, (2) C_3, (3) C_4.

With an increase of J the spectrum of the Hamiltonian (8) shows the transition from the structure appropriate for $\mathbf{R}^{4(4,A_1)}$ to that for $\mathbf{R}^{6(6,A_1)}$. But it should be noted (*15, 23*) that for real molecules $u_0^{4(4,A_1)} \gg u_0^{6(6,A_1)}$ and the critical phenomena could take place at unrealistically high values of J. For excited vibrational states the relations

TABLE I

Coriolis Interaction Parameters and the Vibrational Frequency Difference for the ν_2, ν_4 Bands of Tetrahedral Molecules.

Molecule	$^{12}CH_4$	$^{12}CD_4$	$^{28}SiH_4$	$^{74}GeH_4$	$^{120}SnH_4$	*
Δ cm^{-1}	222.57	93.78	56.97	109.21	72.64	0
$u_{2,4}^{1(1,F_1)}/u_{4,4}^{1(1,F_1)}$	-0.9310	-1.3794	-0.9275	-0.6894	-0.6889	$-2^{\frac{1}{2}}$

* Denotes the case of the $SO(3)$ symmetry.

between parameters are strongly modified due to a larger number of rovibrational resonances. New types of rovibrational tensor operators should be introduced for degenerate and resonant vibrational states. The cluster structure of the spectra of some individual rovibrational tensor operators is studied in Refs. (*3, 4*) for isolated vibrational states of E and F_2 symmetry species. To study critical phenomena the model operators must include at least two tensors of different rank. In Refs. (*16, 25*) the critical phenomenon was studied for a model Hamiltonian of the E-state, which includes as its two most important tensor contributions

$$\mathbf{H} = u_{2,2}^{2(2,E)}\mathbf{U}_{2,2}^{2(2,E)} + u_{2,2}^{3(3,A_2)}\mathbf{U}_{2,2}^{3(3,A_2)}. \tag{9}$$

For real tetrahedral molecules, such as CH_4 and SiH_4, the critical phenomenon predicted in Ref. (*16*) takes place for the ν_2 state at $J \sim 10$–20. Let us analyze this phenomenon for $^{120}SnH_4$ as an example.

The rotational structure of the ν_2 state of $^{120}SnH_4$ is shown in Fig. 3. It is calculated from the parameters obtained in Ref. (*13*). Two branches are clearly shown in Fig. 3. The upper E^- branch includes $(2R + 1)$ levels with $R = J - 2$ and the lower E^+ branch includes $(2R + 1)$ levels with $R = J + 2$. The regrouping of the 6-fold cluster between the E^+ branch and the ν_4 state (see Sec. 3) takes place for this molecule at very high J values. Thus, for the study of diabolic points the present example is not interesting and we consider the critical phenomena only.

At low J values ($J < 10$) the rotational multiplets of both branches possess a cluster structure similar to that of the ground vibrational state. Figure 4 shows that there are two stable stationary rotation axes, C_4 and C_3, and one unstable stationary axis, C_2. For the quantum problem one can see only 6-fold clusters because at low J values the number of quantum levels is rather small to produce all kinds of clusters and the relative stability of the C_3 rotation axis (characterized by the Hessian value) is much smaller than that of the C_4 rotation axis. The Hessian for the C_2 rotation axis becomes positive at $J > 7$ for the E^- branch and at $J > 10$ for the E^+ branch. In accordance with the general consideration (*8*) the nonlocal critical phenomenon with C_2 broken symmetry takes place. The saddle point on the rotational energy surface transforms into a maximum (as on the E^+ surface) or a minimum (as on the E^- surface) and two new unstable stationary points (saddle points). As can be seen from Fig. 4, the Hessian value for the C_2 point of the E^+ rotational surface increases with J and the 12-fold cluster appears in the higher part of the E^+ branch at $J > 14$. The Hessian

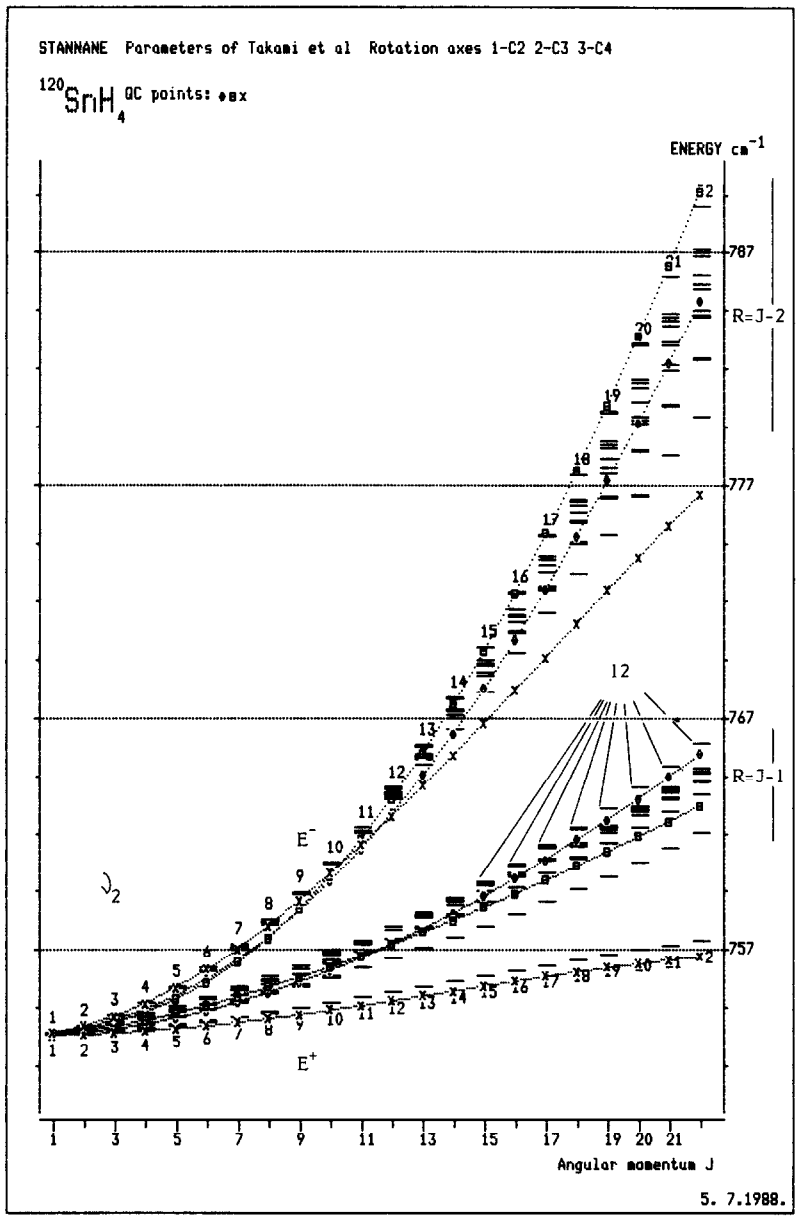

FIG. 3. The rotational structure of the ν_2 state of $^{120}SnH_4$ calculated with the parameters of Ref. (*13*). The dashed line shows the classical rotation energy around stationary axes: (1) C_2, (2) C_3, (3) C_4. See also the note to Fig. 1.

variation for the C_3 rotation axis shows the existence of the C_3 nonlocal critical phenomenon for both branches. It consists of transforming (for the E^+ branch as an example) the local maximum into a minimum at $J = 14$.

The behavior of the Hessian for the C_4 axis is rather different for the E^+ and E^-

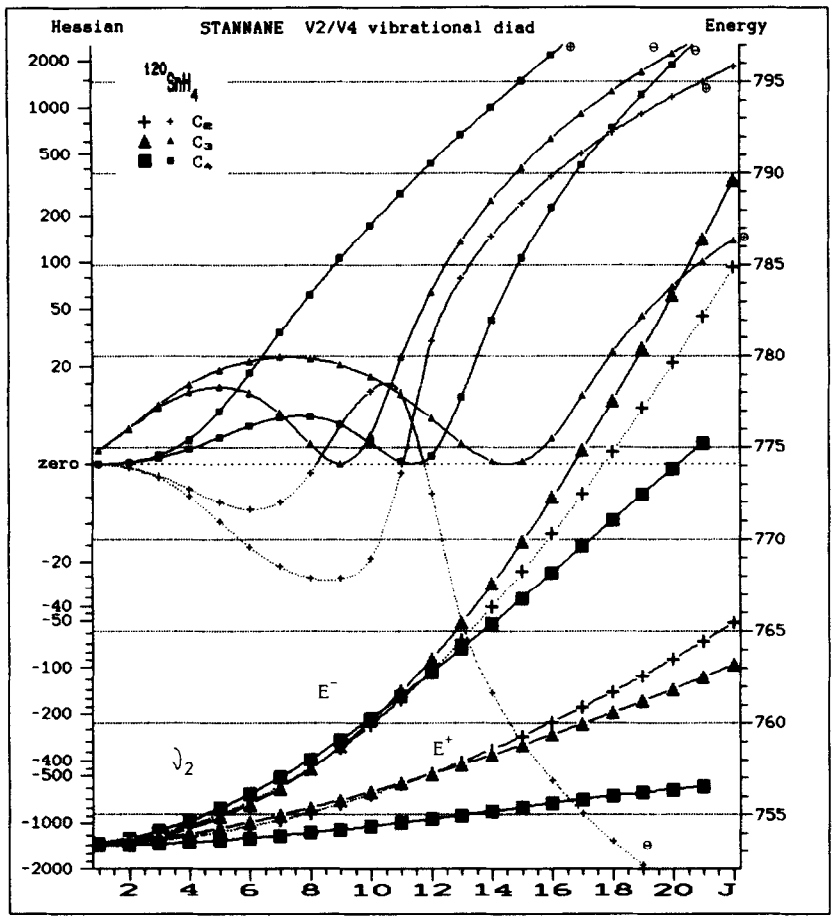

FIG. 4. The bifurcation analysis of the ν_2 band of $^{120}SnH_4$. The signs $\oplus$ and $\ominus$ are used to designate the branches and energy surfaces: + is for the lower branch, E^+ ($R = J + 2$); − is for the upper branch, E^- ($R = J - 2$). *Note*: Large marks correspond to the classical rotation energy. Small marks denote the Hessian values. The stable stationary axes are designated by solid lines, whereas dotted lines are used for the unstable ones. The nonlinear transformation $h(J) \rightarrow \text{arcsh}(\text{const}\ h(J))$ is used to properly represent the Hessian behavior. The marked points are obtained from straightforward classical calculation. The lines are plotted using the Lagrange interpolation.

surfaces. The stability of the C_4 stationary point on the E^+ surface increases with J and the corresponding minima become deeper. The E^- surface shows at the C_4 point the nonlocal critical phenomenon ($J \sim 11$) corresponding to transformation of the local maximum into the minimum. At a slightly higher value of J ($J \sim 12$) the C_2 local critical phenomenon takes place on this surface. This phenomenon corresponds to the change of stability of the C_2 points and disappearance of additional saddle points. These saddle points were born by C_{2v} nonlocal critical phenomena. Then they changed their positions with increasing J and passed through the C_3 and C_4 points causing nonlocal critical phenomena. Finally, these saddle points return to the C_2 points and disappear by the C_2 nonlocal critical phenomenon. As all these critical phenomena take place approximately at the same J value, they may be considered as

one complicated qualitative phenomenon. The resulting modification of the cluster structure of the E^- branch may be represented as an overcrossing of the rotational multiplet taking place at $J \sim 9$–12. For these values of J the E^- energy surface is almost spherical. As a consequence, the rotational splitting is anomalously small at $J \sim 9$, 10 (see Fig. 3). For higher J values the 6-fold and 8-fold clusters are formed in lower and upper parts of the E^- rotational multiplet, respectively.

In conclusion, we want to point out the good agreement between the classical description and the quantum results shown in Fig. 3. The most interesting example of this agreement is the formation of 12-fold clusters in the upper part of the E^+ branch. These clusters verify at the same time the appearance of the critical phenomenon. They were observed experimentally as shown in Table I of Ref. (*13*), where $Q(14)$ transitions to the ν_2 levels forming a 12-fold cluster (E, F_1, F_1, F_2, A_2) are listed. In the $^{120}SnH_4$ spectrum these transitions are observed in the frequency range of 759.0881–759.1776 cm^{-1}, whereas the nearest line is situated at 758.6712 cm^{-1}. Figure 3 indicates that the cluster cited above is probably the first 12-fold cluster occurring in the ν_2 state of $^{120}SnH_4$. It should be noted that we use the relation of Ref. (*24*)

$$u_{2,4}^{2(2,F_2)} = -(3/2)^{1/2} d_{2,4} \tag{10}$$

to reproduce the structure of the rotational multiplet by means of the parameters obtained in Ref. (*13*).

5. QUALITATIVE ANALYSIS OF THE ROTATIONAL STRUCTURE OF THE ν_1, ν_3 DYAD OF $^{120}SnH_4$

The characteristic feature of the vibrational spectra of stannane is the small splitting (~ 2 cm^{-1}) of the ν_1 and ν_3 stretching vibrations. Such quasidegeneracy is typical for tetrahedral molecules with a heavy central atom (SiH_4, GeH_4). Thus, the treatment of the ν_1, ν_3 bands as an isolated dyad seems to be adequate. At the same time, it should be noted that the internal structure of the ν_1, ν_3 dyad changes considerably when passing from SiH_4 to GeH_4 and SnH_4, due to strong variation of the Coriolis interaction. The Coriolis constant $B\zeta_3$ for the ν_3 state has a small positive value for SiH_4 and takes large negative values for GeH_4 and SnH_4. Moreover, the isotopic shift of the ν_3 band is of the same order of magnitude as the ν_1, ν_3 frequency difference $\Delta = \nu_1 - \nu_3$. So the rotational structure of the ν_1 and ν_3 bands may vary considerably with isotopic substitution. We studied the peculiarities of the ν_1, ν_3 bands of $^{28}SiH_4$ earlier (*16*). In this section, we present a qualitative theoretical analysis of the rotational structure of ν_1, ν_3 bands of $^{120}SnH_4$ studied experimentally in the recent work of Krivtsun *et al.* (*14*). This experimental study was especially devoted to the investigation of those parts of the energy level structure where the qualitative phenomena should exist.

The set of spectroscopic parameters for the ν_1, ν_3 dyad found from the experimental data (*14*) enables one to reproduce the energy-level system at $J = 1, \ldots, 16$ with an accuracy of about 0.002–0.005 cm^{-1}. The rotational structure of the ν_1, ν_3 dyad of $^{120}SnH_4$ is qualitatively different from that of $^{28}SiH_4$. The ν_3 band of $^{120}SnH_4$ possesses three clearly seen branches denoted usually as F^-, F^0, F^+. They are split by a large Coriolis interaction $B\zeta_3 = -6^{1/2} u_{3,3}^{1(1,F_1)}$.

Let us now discuss the results of the (semi)classical qualitative analysis of the ν_1 and ν_3 states. The energies of the stationary points of the rotational energy surfaces

are plotted in Fig. 5 along with the system of quantum energy levels. The classical analysis shows the existence of several critical phenomena and diabolic points. The F^0 branch exhibits the C_2 nonlocal critical phenomenon. The comparison of Fig. 6 with Fig. 4 shows that this critical phenomenon is just the same as that studied in Sect. 4 in the E^+ branch of the ν_2 band. As seen from Figs. 5 and 6, the F^0 energy

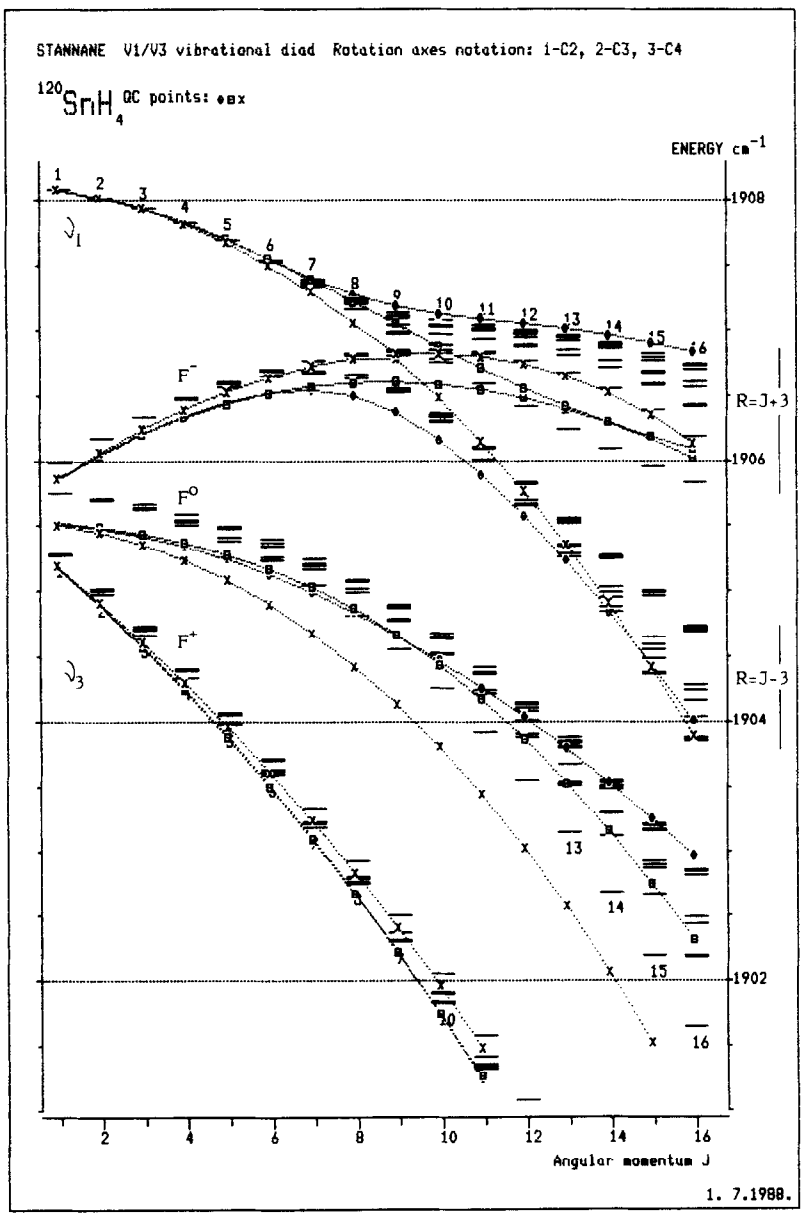

FIG. 5. The rotational structure of the ν_1, ν_3 dyad of $^{120}SnH_4$ according to Ref. (*14*). The dashed lines show the energy of classical rotation around stationary axes: (1) C_2 (rhomb), (2) C_3 (square), (3) C_4 (cross). See also the note to Fig. 1.

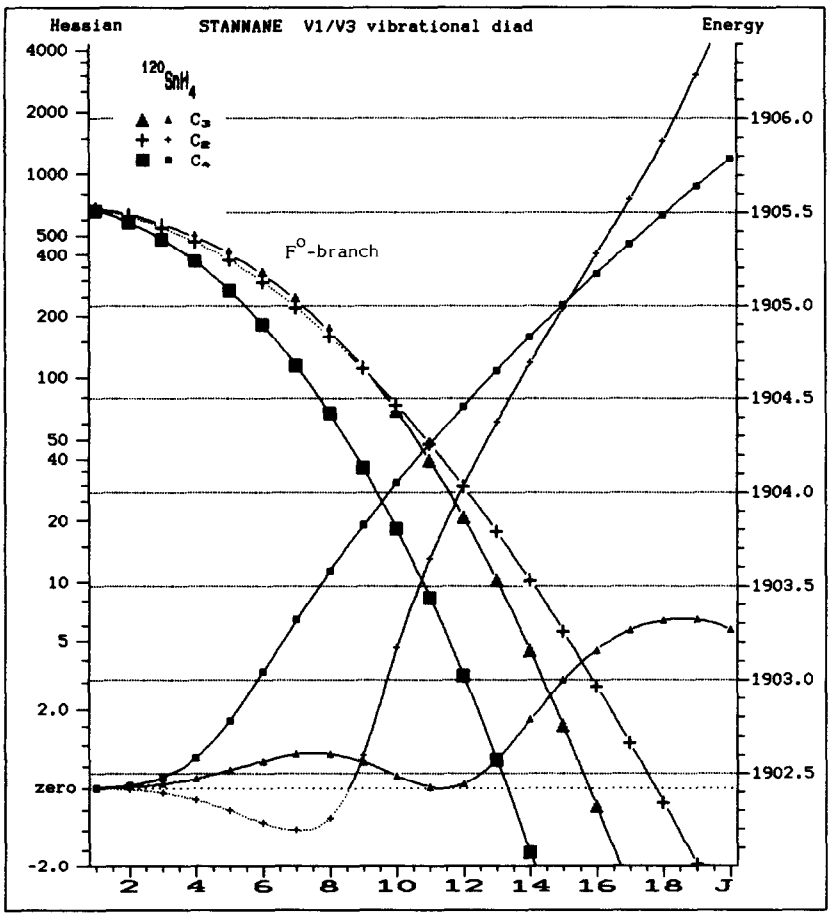

FIG. 6. The bifurcation analysis of the ν_3 F^0 branch of $^{120}SnH_4$. See the note to Fig. 4.

surface has a deep minimum in the C_4 direction. The corresponding localized states forming the 6-fold clusters lie in the lower part of the F^0 branch and are well seen in the IR Q-branch spectrum of ν_3. We indicate as an example the lines 50, 51, 57, 73, 83 in Fig. 4 and Table II of Ref. (*14*). For low J values there are no localized states in the upper part of the F^0 multiplet because the C_2 rotation axis is unstable and stability of the C_3 rotation is too small (the corresponding Hessian value is positive but rather small). With increasing J the C_2 rotation axis becomes stable at $J \sim 9$. The corresponding maxima on the energy surface grow with J and become global for $J > 11$. Such a transformation is accomplished with the formation of 12-fold clusters in the upper part of the F^0 multiplet. The first cluster of this type is clearly seen in Fig. 5 for $J = 13$. It was experimentally observed in the Q-branch of the ν_3 band: see lines 78, 79 in Table II of Ref. (*14*).

Similarly to the critical phenomenon in the ν_2 band, the increase of the stability of the C_2 rotation is associated with the decrease of the C_3 rotation stability. At $J \sim 11$ the Hessian for the C_3 axis goes to zero and the C_3 nonlocal critical phenomenon takes place. It results in the formation of a minimum in the C_3 direction instead of a

maximum. The saddle points which appear at $J \sim 9$ near the C_2 axis and participate in the C_3 critical phenomenon at $J \sim 11$ are not shown in Figs. 4, 5, 6 for the sake of simplicity. The variation of the saddle point positions with increasing J was studied earlier in detail for some model problem (*16, 25*).

The simple classical approach enables us to study the rotational dynamics close to diabolic points as well. For the ν_1, ν_3 dyad of $^{120}SnH_4$ such a peculiarity arises between ν_1 and the F^- branch of ν_3. The ν_1 band is situated higher in energy than the F^- one at $J < 9$. The ν_1 and F^- rotational surfaces possess respectively minima and maxima in the C_4 direction. The 6-fold cluster is well-pronounced in the upper part of the F^- multiplet. This cluster is clearly seen in the R-branch spectra [see lines 55, 56 ($J = 6$); 77 ($J = 7$); 111, 96 ($J = 8$); and 127, 128, 129 ($J = 9$) in Figs. 3, 4 and Table II of Ref. (*14*)]. For $J \sim 9$ two energy surfaces (ν_1 and F^-) form one two-sheet surface with six equivalent diabolic points in the C_4 direction. Figure 7 shows that the Hessian goes to infinity under diabolic point formation. Passing through the diabolic point corresponds to the transition of the 6-fold cluster from the lower surface to the upper one. The wave functions of the states at $J \sim 9$–10 have a mixed ν_1, ν_3 character. As J increases, the ν_1 band, which is now below the F^- branch, becomes more pure and the probabilities of the transitions to this band decrease (see Fig. 8).

Special attention should be paid to the sequence of the 8-fold clusters, which are located near the extreme value of the C_3 classical rotation energy at $J = 10 \cdots 16$. Figures 5 and 7 show that these energies for both surfaces are very close at $J = 10, \ldots, 16$ and the diabolic point is formed at $J \sim 14$. The Hessian for the C_3 points is large and the existence of a quantum state with the energy close to the diabolic point may be due only to "quantum tunneling" between two different energy surfaces. Thus, the resulting localized quantum states are highly mixed and the corresponding transitions to these states are rather intense. At the same time, the calculation of the IR transition probabilities given in Fig. 8 shows that the R-branch transitions are even more forbidden than the corresponding ν_1 transitions for high J. This cluster exhibits the anomalous property in the Q-branch, where the transition probabilities are almost two orders larger than those of the forbidden ν_1 and F^- bands (see Fig. 8). The discussed sequence of 8-fold clusters lies about 1 cm^{-1} above the $J = 1$ level of the F^0 branch and the corresponding spectrum is clearly seen on the blue side of the allowed Q-branch of the ν_3 band. Figure 9 shows the part of the experimental spectra (*14*) including the $Q(10), \ldots, Q(14)$ lines. The small isotopic shift of these lines verifies the large contribution of the ν_1 vibration to corresponding states. At the same time, the 8-fold clusters lie very close in energy to the reformed F^- branch, which includes $(2J + 7)$ rotational levels at $J > 12$ (the formal pseudorotational quantum number $R = J + 3$ may be used for this branch). This branch is characterized by a rich cluster structure which includes a 12-fold cluster in the upper part of the multiplet and both 6-fold and 8-fold ones in the lower part, in complete agreement with classical analysis.

After intersection with the F^- band, the ν_1 band includes $(2J - 5)$ rotational levels only. Thus, the psuedorotational quantum number $R = J - 3$ may be used for this band designation. In contrast to the F^- branch there exist a number of delocalized quantum states in the ν_1 band at $J = 10, \ldots, 16$ due to the small Hessian value at the C_2 and C_4 points on the corresponding energy surface. Moreover, Fig. 7 shows that the C_4 nonlocal critical phenomenon takes place at $J \sim 13$ and the C_2 rotation

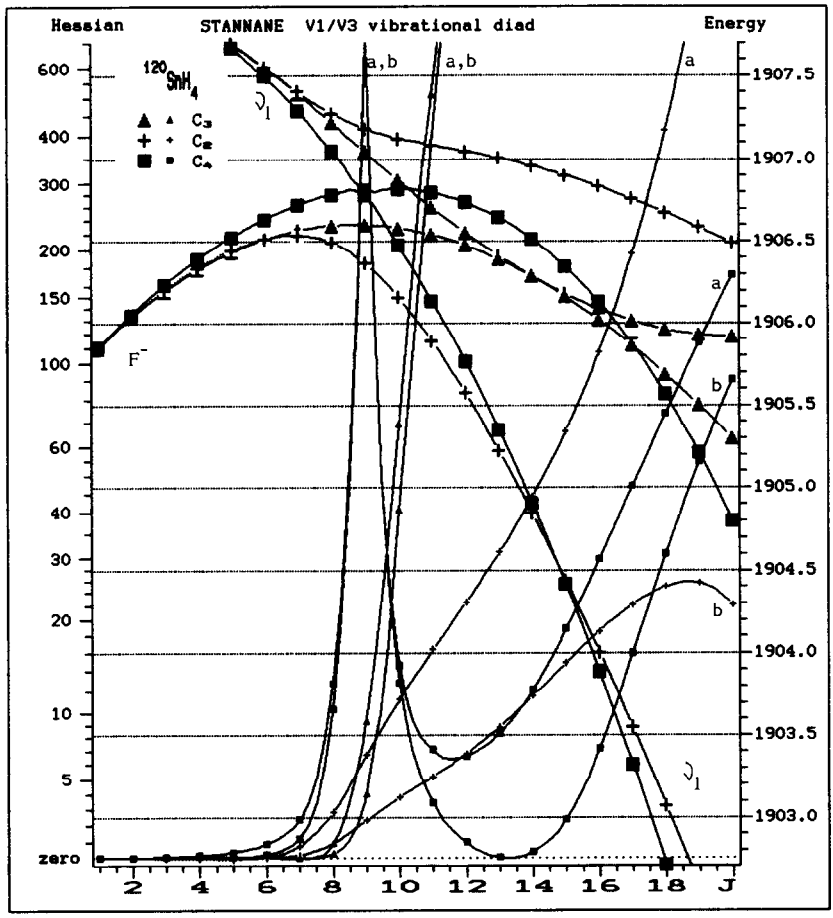

FIG. 7. The bifurcation analysis of two upper branches of the ν_1, ν_3 dyad of $^{120}SnH_4$: the ν_1 band and the F^- branch of ν_3. The upper branch is denoted by a and the lower one by b. See the note to Fig. 4.

becomes unstable again at $J \sim 25$. Such organization of critical phenomena would complete the overcrossing of the ν_1 band similarly to that of the $\nu_2(E^-)$ branch discussed above.

One may estimate on the basis of the parameters reported in Ref. (*14*) that the intersection of the ν_1 and F^0 branches should occur when J increases. But the accuracy of the parameters is not sufficient to make a definite conclusion about the rotational structure of the ν_1, ν_3 bands for $J > 20$. Thus, the highly excited rotational states of the ν_1, ν_3 bands require further experimental and theoretical study. The ν_1 band for $J > 12$, the evolution of 8-fold clusters in the F^- band for $J > 16$, and relative positions of the F^0 and ν_1 bands at high J values are of primary interest.

6. CONCLUSION

The main purpose of the present article was to demonstrate the simplicity and efficiency of classical qualitative analysis of concrete molecular systems. The classical description enables one to clearly understand the rovibrational dynamics in rather

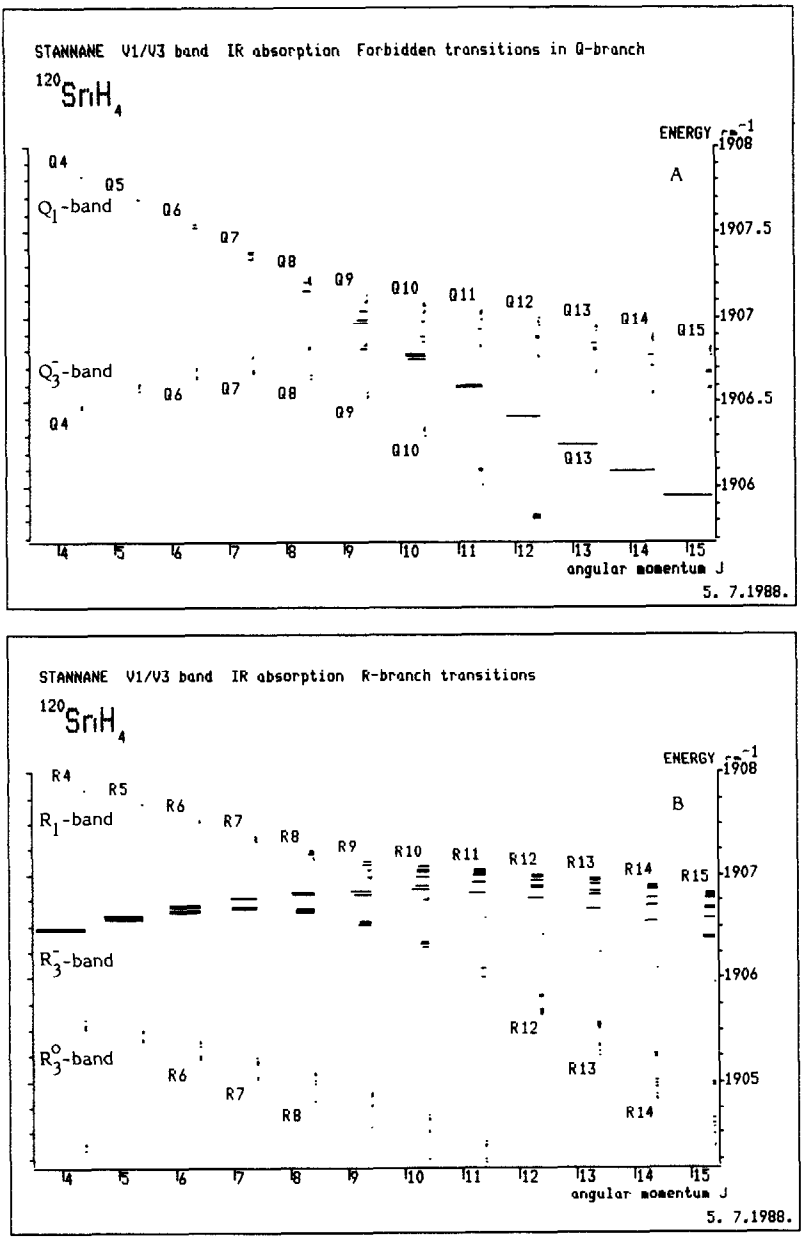

FIG. 8. Relative intensities in the ν_1, ν_3 absorption spectrum of $^{120}SnH_4$. (A) Forbidden transitions in the Q branch (the Q_1 and Q_3^- bands). (B) allowed transitions in the R_3^- branch and forbidden transitions for the R_3^o and R_1 branches. *Note*: The transition probability to a given energy level was obtained as a sum over the ground state levels. It corresponds to the length of the line designating the level. In each figure the reduced matrix element was not taken into account and the normalization was done with respect to the most intense transition. See also the note to Fig. 1.

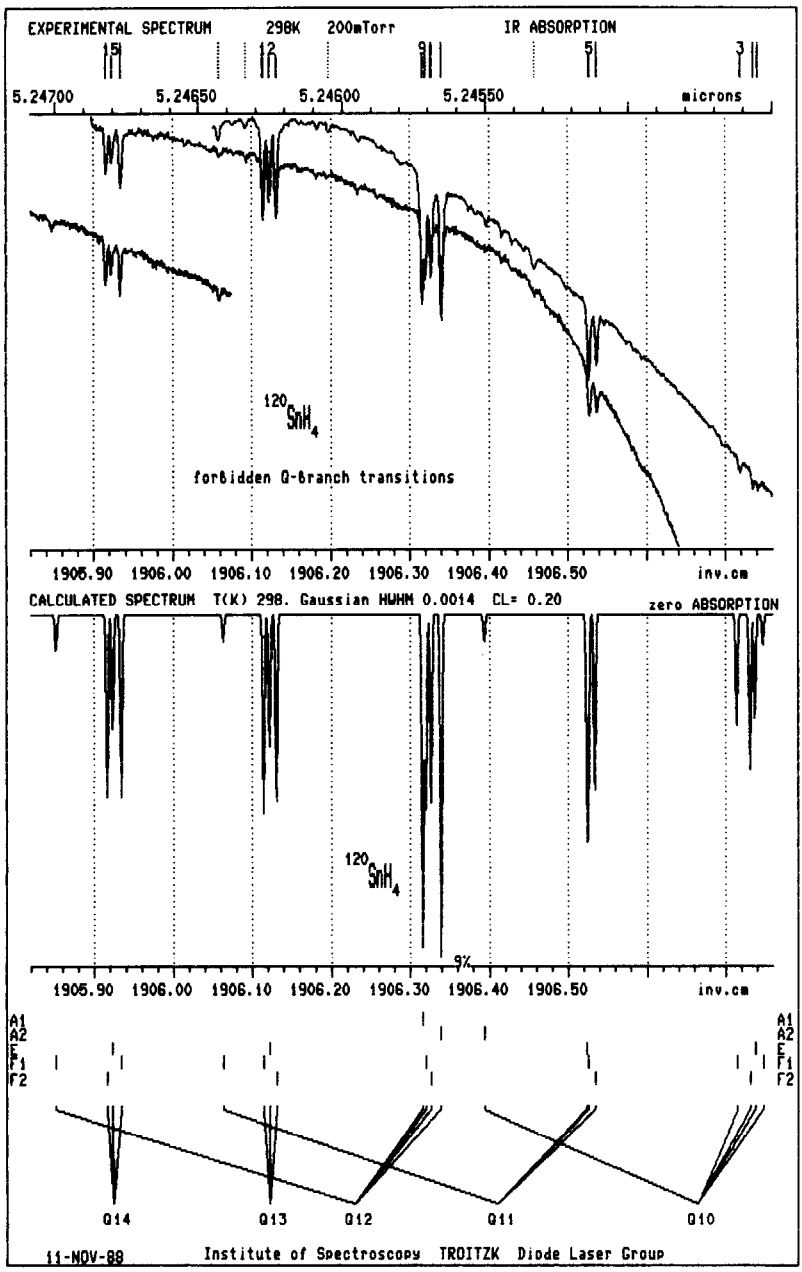

FIG. 9. A fragment of the absorption spectrum of the forbidden Q-branch of the ν_1 band. The assignment of the theoretical spectrum is shown for the sequence of 8-fold clusters discussed in Section 5. The experimental spectrum was obtained in Ref. (*14*).

complicated cases. It seems to be ultimately useful for the study of more highly excited rovibrational states. The location of qualitative changes in the rotational structure (both critical phenomena and diabolic points) can indicate the most interesting energy

regions for further experimental study and even give some ideas on the more adequate construction of the effective Hamiltonians taking into account the universal Hamiltonians for different critical phenomena (*8*). It should be noted that the theory of critical phenomena (*8*) and the interpretation of the diabolic points (*12, 16*) as well are phenomenological approaches similar to the Landau theory of second-order phase transitions in macroscopic physics. The open problem now is the development of the microscopic theory of qualitative changes in finite-particle systems which would relate them with intramolecular dynamics. This problem is closely connected to transformation of effective spectroscopic parameters to molecular constants.

APPENDIX: ROVIBRATIONAL TENSOR OPERATORS INVARIANT WITH RESPECT TO THE $SO(3)$ GROUP

Let us consider five vibrational annihilation (creation) operators for the ν_2 and ν_4 modes as components of the spherical tensor operator of rank 2:

$$\mathbf{V}^{(2)} = (\mathbf{a}_1^E, \mathbf{a}_2^E, \mathbf{a}_x^{F_2}, \mathbf{a}_y^{F_2}, \mathbf{a}_z^{F_2}). \tag{A-1}$$

Supposing now that the rovibrational Hamiltonian for the ν_2, ν_4 dyad must be $SO(3)$ invariant, we can represent any such operator in the form

$$[^s[\mathbf{V}^{+(2)} * \mathbf{V}^{(2)}]^{(K)} * \mathbf{R}^{\Omega(K)}]^{(0)}, \qquad s = (-1)^K, \tag{A-2}$$

where K is the rank with respect to the $SO(3)$ group. In order to relate the operators (A-2) with that constructed in the coupling scheme for the cubic symmetry group it is natural to use the chain of groups $SO(3) \supset 0$. In this case we have for the vibrational operators the form

$$(\mathbf{V}^{+(2)} * \mathbf{V}^{(2)})_p^K = (-1)^K (2K+1)^{1/2} [p]^{-1/2} \sum_{p',p''} K \begin{pmatrix} 2 & 2 & K \\ p' & p'' & p \end{pmatrix} (\mathbf{V}_{p'}^{+(2)} * \mathbf{V}_{p''}^{(2)}), \tag{A-3}$$

where $K\left(\begin{smallmatrix} J' & J'' & J \\ p' & p'' & p \end{smallmatrix}\right)$ is the isoscalar factor for the chain of groups considered (*26*). According to (A-3) the $SO(3)$-invariant Hamiltonian of the harmonic oscillator includes only the term

$$\mathbf{H}_0 = (5)^{-1/2} \sum_{G=E,F_2} \sum_{s=1\cdots[G]} ((\mathbf{a}^+)_s^G (\mathbf{a})_s^G). \tag{A-4}$$

The part of the ν_2, ν_4 Hamiltonian linear in rotational angular momentum operators includes only one $SO(3)$ invariant tensor,

$$\mathbf{H}_1 = ((\mathbf{V}^{+(2)} * \mathbf{V}^{(2)})^{(1)} \mathbf{R}^{1(1)})^{(0)} = 5^{-1/2}[(((\mathbf{a}_4^+)^{F_2} (\mathbf{a}_4)^{F_2})^{F_1} - 2^{1/2} \ominus ((\mathbf{a}_2^+)^E (\mathbf{a}_4)^{F_2})^{F_1}) * \mathbf{R}^{1(1,F_1)}]^{A_1} = 5^{-1/2}[\mathbf{U}_{4,4}^{1(1,F_1)} - 2^{1/2} \mathbf{U}_{2,4}^{1(1,F_1)}]. \tag{A-5}$$

The expression (A-5) is the Coriolis interaction for the ν_2, ν_4 dyad under the supposition of the $SO(3)$ invariance. It should be mentioned that the approximate classification of the rotational states and the construction of the irreducible tensor operators, taking into account an additional classification with respect to the irreducible representations of the $SO(3)$ group, have been discussed repeatedly in the literature (*27*).

RECEIVED: December 14, 1988

REFERENCES

1. A. J. DORNEY AND J. K. G. WATSON, *J. Mol. Spectrosc.* **42,** 135–148 (1972).
2. W. G. HARTER AND C. W. PATTERSON, *J. Chem. Phys.* **66,** 4872–4885 (1977); C. W. PATTERSON AND W. G. HARTER, *J. Chem. Phys.* **66,** 4886–4892 (1977).
3. W. G. HARTER, C. W. PATTERSON, AND H. W. GALBRAITH, *J. Chem. Phys.* **69,** 4896–4907 (1978).
4. W. G. HARTER, H. W. GALBRAITH, AND C. W. PATTERSON, *J. Chem. Phys.* **69,** 4888–4895 (1978).
5. W. G. HARTER, C. W. PATTERSON, AND F. J. DA PAIXAO, *Rev. Mod. Phys.* **50,** 37–83 (1978).
6. W. G. HARTER AND C. W. PATTERSON, *J. Chem. Phys.* **80,** 4241–4261 (1984).
7. W. G. HARTER, *Phys. Rev. A* **24,** 192–263 (1981); W. G. HARTER AND C. W. PATTERSON, *Phys. Rev. A* **19,** 2277–2303 (1979).
8. B. I. ZHILINSKII AND I. M. PAVLICHENKOV, *Zh. Eksp. Teor. Fiz.* **92,** 387–403 (1987) in Russian; *Sov. Phys. JETP Engl. Transl.* **65,** 221–229 (1987); *Sov. Phys. Dokl. Engl. Transl.* **31,** 423–425; I. M. PAVLICHENKOV AND B. I. ZHILINKSII, *Ann. Phys. (N.Y.)* **184,** 1–32 (1988).
9. I. M. PAVLICHENKOV AND B. I. ZHILINSKII, *Chem. Phys.* **100,** 339–354 (1985).
10. M. V. BERRY, *Proc. R. Soc. London, Ser. A* **392,** 45–57 (1984); M. V. BERRY AND R. J. MONDRAGON, *J. Phys. A: Math. Gen.* **19,** 873–885 (1986).
11. R. JACKIW, *Comments At. Mol. Phys.* **21,** 71–82 (1988) and references therein.
12. V. B. PAVLOV-VEREVKIN, D. A. SADOVSKII, AND B. I. ZHILINSKII, *Europhys. Lett.* **6,** 573–578 (1988).
13. Y. OSHIMA, Y. MATSUMOTO, M. TAKAMI, S. YAMAMOTO, AND K. KUSHITSU, *J. Chem. Phys.* **87,** 5141–5148 (1987).
14. V. M. KRIVTSUN, D. A. SADOVSKII, E. P. SNEGIREV, A. P. SHOTOV, AND I. I. ZASAVITSKII, *J. Mol. Spectrosc.* **139,** 107–125 (1990).
15. B. I. ZHILINSKII, V. I. PEREVALOV, AND VL. G. TYUTEREV, "The Irreducible Tensor Operator Method in the Theory of Molecular Spectra," Chap. 7, Nauka, Novosibirsk, 1987 [in Russian].
16. D. A. SADOVSKII AND B. I. ZHILINSKII, *Mol. Phys.* **65,** 109–128 (1988).
17. H. A. JAHN, *Proc. R. Soc. London Ser. A* **168,** 495–518 (1938).
18. D. L. GRAY AND A. G. ROBIETTE, *Mol. Phys.* **32,** 1609–1625 (1976); J.-P. CHAMPION, *Canad. J. Phys.* **55,** 1802–1828 (1975); J.-P. CHAMPION AND G. PIERRE, *J. Mol. Spectrosc.* **79,** 255–280 (1980).
19. W. A. KREINER AND A. G. ROBIETTE, *Canad. J. Phys.* **57,** 1969–1981 (1979).
20. G. HERZBERG, "Infrared and Raman Spectra of Polyatomic Molecules," Van Nostrand, New York, 1945.
21. L. D. LANDAU AND E. M. LIFSHITZ, "Quantum Mechanics," Pergamon, Oxford, 1965.
22. L. C. BIEDENHARN AND J. D. LOUCK, "Angular Momentum in Quantum Physics. Theory and Applications," Addison-Wesley, Reading, MA, 1981.
23. W. G. HARTER AND C. W. PATTERSON, *J. Math. Phys.* **20,** 1453–1459 (1979).
24. D. A. SADOVSKII AND B. I. ZHILINSKII, *J. Mol. Spectrosc.* **115,** 235–257 (1986).
25. B. I. ZHILINSKII AND D. A. SADOVSKII, *Opt. Spektrosk.* **61,** 481–486 (1986) [in Russian]; *Opt. Spectrosc. Engl. Transl.* **61,** 301–304 (1987).
26. J.-P. CHAMPION, G. PIERRE, F. MICHELOT, AND J. MORET-BAILLY, *Canad. J. Phys.* **55,** 512–520 (1977).
27. H. BERGER, *J. Mol. Spectrosc.* **55,** 48–55 (1975); F. MICHELOT, *J. Mol. Spectrosc.* **63,** 227–240 (1976), **67,** 62–92 (1977); D. B. LITVIN AND K. FOX, *J. Chem. Phys.* **76,** 3908–3912 (1982).